ISSN (Print) 1226-1750
ISSN (Online) 2233-6656
Journal of Magnetics 23(4), 491-498 (2018) https://doi.org/10.4283/JMAG.2018.23.4.491

Simultaneous Effects of Slip and Wall Stretching/Shrinking on Radiative Flow of Magneto Nanofluid Through Porous Medium

A. Zeeshan[1]*, H. F. Ismael[2], M. A. Yousif[2], T. Mahmood[3], and S. U. Rahman[4]

[1]*Department of Mathematics and Statistics, FBAS, International Islamic University, Islamabad, Pakistan*
[2]*Faculty of Science, Department of Mathematics, University of Zakho, Kurdistan Region, Iraq*
[3]*Department of Electronics Engineering, University of Engineering and Technology Taxila sub Campus Chakwal, Pakistan*
[4]*Department of Computer Science, University of Engineering and Technology Taxila sub Campus Chakwal, Pakistan*

(Received 8 June 2018, Received in final form 13 October 2018, Accepted 16 October 2018)

Effects of the uniform magnetic field on aqueous magneto-Nanofluid confined in a porous domain with wall stretching/shrinking non-linearly is analyzed via this communication. The problem is modeled using continuity, momentum and energy equation along with linear thermal radiation. The effects of physical quantities are observed for Cu, Al_2O_3, TiO_2 and Ag particles in water. The coupled boundary layer PDE's are reduced into the system of ODEs by utilizing similarity transformation and solved using shooting and Runga-Kutta fourth order technique. Stability of the obtained results are also analyzed. The results are displayed through graphs. It is observed that the momentum boundary layer is thicker when silver particles are introduced in water. Whereas, temperature profile has the minimum value for silver nanoparticles and maximum for Titanium dioxide. Also, in case of shrinking sheet dual solutions are obtained along with smallest Eigen values.

Keywords : magnetic Nanofluid, second order slip boundary condition, non-linear stretching/shrinking sheet, porous medium, thermal radiation

1. Introduction

Modern developments have revolutionized into novel engineering nanotechnology, which led to the progress of a new sort of heat transfer fluid called Nanofluid. Nanofluids are used widely in industrial applications including nuclear reactors, transportation industry, engine cooling, hyperthermia, biomedicine, vehicle technology, solar water heating and heat exchanger. Nanofluids gain rapid attention to the researcher for both theoretical and experimental point of view [1-3]. Choi *et al.* [4] was the first one who gave the idea of Nanofluid comprising of solid nanoparticles with size approximately 10 nm. Nano-Fluids are dilute suspended metallic particles (gold, titanium, copper, iron and their oxides) into conventional fluids like water, ethylene glycol, oil and lubricants [5]. Eastman *et al.* [6] have verified experimentally that the thermal conductivity of the nanoparticles is greater than conventional fluids. Li *et al.* [7] demonstrated that for a lower concentration of nanoparticles typically (< 5%), the thermal conductivity of the conventional fluid is improved by 10-20%. Sheikholeslami *et al.* [8] sees the influence of magnetic field on Nanofluid. Baby and Ramaprabhu [9] have studied the Nanofluids comprising graphene for thermal conductivity and heat transfer. Bachok *et al.* [10] inspected the Nanofluid flow over a moving semi-infinite flat surface with the hypothesis that the plate moves in the same or reverse directions to free stream. Makinde and Aziz [11] have demonstrated the influence of convective boundary condition and heat transport flow over a stretch-able surface fill with Nanofluid. Zeeshan *et al.* [12] dis-cussed the effect of magnetization of the ferromagnetic nanoparticle in water. The effects of aggregation of nano-particles are discussed by Ellahi *et al.* [13]. The entropy generation due to the presence of nanoparticles in the fluid over a revolving plate is discussed by Rashidi *et al.* [14].

The discussion regarding the magnetization effect has imperative presentations in the field of physics, chemistry, industrial and engineering stuff, like MHD generators, bearings, pumps, and boundary layer control are exagge-rated by the association among the magnetic field and

*Corresponding author: Tel: +92-51-901-9732
e-mail: ahmad.zeeshan@iiu.edu.pk

electrically conducting fluid [15, 16]. Ganga *et al.* [17] investigated the viscous and Ohmic dissipations on magnetohydrodynamic radiative Nanofluid flow over a vertical plate along with internal heat generation or absorption. Some recent studies on for Nanofluid flowing through uniform and non-uniform magnetic field are listed in [18-22].

Furthermore, in micro-electro-mechanical systems, the fluid flow behaviour does not obey the no-slip boundary condition. So, slip conditions are necessary in order to illuminate the fluid flow. When the fluids composed of distinct particles like suspensions, foams, polymer solutions and emulsions, partial slip may take place across a moving surface. Slip flow has tremendous applications like the smoothening of internal cavities and artificial heart shells. Turkyilmazoglu [23] analyzed MHD second-order slip model and heat transport flow over a permeable stretching or shrinking surfaces. Rosca and Pop [24] explored the influence of slip on boundary layer flow of micropolar fluid past a shrinking sheet.

The motion of charged particles in matter generated some electromagnetic radiation called thermal radiation. Some common examples of radiation include the cosmic microwave background radiation and light emitted by a bulb etc. Applications and importance of radiations indulge many scientists to explore the concept of radiation in MEMS and NEMS [25-27].

Nanotechnology is considered a significant force that will drive a revolution in industries and technology. Nanofluids represents the cutting edge in heat transfer and many technological advancements from space technology to medical engineering. Motivated by the diverse applications of these fluids, the emphasis of the current article is placed on Copper (Cu), Alumina (Al_2O_3), Titanium oxide (TiO_2), Silver (Ag) nanosize particles placed in an aqueous medium flowing over a non-linearly stretching sheet is observed. A uniform magnetic field is applied perpendicular to the flow. The wall offers second-order momentum slip. Problem is formulated, and similarity transforms is used to convert coupled partial differential equation into nonlinear ordinary differential equations. Effect of physical parameters on all four Nanofluid is presented on velocity and temperature profile in form of graphs. Finally, some important observations are concluded.

2. Mathematical Formulation

2.1. Stretching/Shrinking sheet

The continuity, Naiver-Stokes and heat equations for incompressible electrically conducting viscous magneto-Nanofluid over a thin sheet is employed for modeling the problem. The magnetic field of strength B_0 normal to the sheet is applied. The base fluid is considered as water. Covering boundary-layer equations are:

$$u_x + v_y = 0 \tag{1}$$

$$uu_x + vu_y = \nu_{nf} u_{yy} - \frac{\sigma B^2(x)}{\rho_{nf}} u - \frac{\nu_{nf}}{k_*'(x)} u \tag{2}$$

$$(\rho c_p)_{nf}(uT_x + vT_y) = \alpha_{nf} T_{xx} - q_{ry} \tag{3}$$

The associative boundary equations for velocity and temperature fields are

$$u = u_w + u_{slip},\ v = 0,\ T = T_w \ \text{ at } y = 0 \tag{4}$$

$$u = 0,\ T \to T_\infty \ \text{ at } \ y \to \infty, \tag{5}$$

Where $u_w = c\sqrt{x^{2n}}$, u and v are components of velocity in the direction of coordinate axis and T is the Nanofluid temperature. The symbols ν_{nf}, ρ_{nf} and σ represents kinematic viscosity, density, and electrical conductivity of Nanofluids $(c_p)_{nf}$, α_{nf} are heat capacity, thermal conductivity, and q_r is the radiative heat flux and given by Quinn Brewster using Roseland approximation,

$$q_r = \left(-\frac{4\sigma^*}{3k^*}\right)(4TT_\infty^3 - 3T_\infty^4)$$

Using the below expression of Nanofluid

$$\rho_{nf} = (1-\phi)\rho_f + \phi\rho_s,\ \mu_{nf} = \frac{\mu_f}{(1-\phi)^{2.5}},$$

$$\frac{\alpha_{nf}}{\alpha_f} = \frac{(\alpha_s + 2\alpha_f) - 2\phi(\alpha_f - \alpha_s)}{(\alpha_s + 2\alpha_f) + 2\phi(\alpha_f - \alpha_s)},$$

$$(\rho c_p)_{nf} = (1-\phi)(\rho c_p)_f + \phi(\rho c_p)_s$$

with stream function transformation, $u = \psi_u$ and $v = -\psi_x$, where

$$\eta(x,y) = \left(\frac{c(n+1)x^{n-1}}{2\nu}\right)^{\frac{1}{2}} y,\ \psi(x,y) = \left(\frac{2\nu c x^{n+1}}{(n+1)}\right)^{\frac{1}{2}} f(\eta),$$

$$T = T_\infty + (T_w + T_\infty)g(\eta) \ \text{ and } \ T_w - T_\infty = (T - T_\infty)x^{2n}$$

we get

$$(1-\phi)^{-2.5} f''' + \left((1-\phi) + \phi\frac{\rho_s}{\rho_f}\right)(ff'' - \beta f'^2)$$

$$-\left(M + \frac{(1-\phi)^{-2.5}}{k_p}\right) f' = 0 \tag{6}$$

$$\left(\frac{\alpha_{nf}}{\alpha_f} + R\right) g'' + Pr\left((1-\phi) + \phi\frac{(\rho c_p)_s}{(\rho c_p)_f}\right)(g'f - f'g) = 0 \tag{7}$$

The boundary condition will reduce into:

$f(0)=0, f'(0)=\lambda+\gamma f''(0)+\delta f'''(0), g(0)=1$ at $\eta=0$ (8)

$f'(\infty)\to 0$, $g(\infty)\to 0$ at $\eta\to\infty$ (9)

k_*' is the porosity variable and it is equal to $k'x^{1-n}$, $u_w=cx^n$, here c is the rate of stretching/shrinking and $u_{slip}=Au_y$ in which $\beta=\frac{2n}{n+1}$, $M=\frac{2\sigma B_0^2}{c_{\rho f}(n+1)}$, $\frac{1}{k_p}=\frac{2\nu_f}{(n+1)ck'}$ $R=\left(\frac{16\sigma^* T_0^3}{3(c_p\mu)_f k^*}\right)$, $Pr=\frac{(c_p\mu)_f}{\alpha_f}$ are the power index, the parameter of magnetic field, the parameter of permeability, the Prandtl and Radiation number respectively. λ is the stretching parameter if $\lambda>0$ and shrinking parameter if $\lambda<0$.

For $n=1$, the momentum and heat equation, with associated boundary condition, takes the formula

$$(1-\phi)^{-2.5}f'''+\left((1-\phi)+\phi\frac{\rho_s}{\rho_f}\right)(ff''-f'^2) - \left(M^*+\frac{(1-\phi)^{-2.5}}{k_p^*}\right)f'=0 \quad (10)$$

$$\left(\frac{\alpha_{nf}}{\alpha_f}+R^*\right)g''+Pr\left((1-\phi)+\phi\frac{(\rho c_p)_s}{(\rho c_p)_f}\right)(g'f-f'g)=0 \quad (11)$$

The boundary condition will reduce to:

$f(0)=0, f'(0)=\lambda+\gamma f''(0)+\delta f'''(0), g(0)=1$ at $\eta=0$ (12)

$f'(\infty)\to 0$, $g(\infty)\to 0$ at $\eta\to\infty$ (13)

The power index $\beta=0$, the parameter of magnetic field is $M^*=\frac{\sigma B_0^2}{c\rho_f}$, the parameter of permeability is $\frac{1}{k_p^8}=\frac{\nu_f}{c_p k'}$, the Prandtl number is $Pr=\frac{(c_p\mu)_f}{\alpha_f}$ and Radiation number is $R^*=\left(\frac{16\sigma^* T_0^3}{3(c_p\mu)_f k^*}\right)$, respectively.

2.2. Stability Analysis

In order to analysis stability, we consider unsteady momentum and temperature profile as defined by [28],

$$u_t+uu_x+vu_y=\nu_{nf}u_{yy}-\frac{\sigma B^2(x)}{\rho_{nf}}u-\frac{\nu_{nf}}{k_*'(x)}u \quad (14)$$

$$T_t+(\rho c_p)_{nf}(uT_x+vT_y)=\alpha_{nf}T_{xx}-q_{ry} \quad (15)$$

With continuity equation together with unsteady similarity transformation,

$$\eta(x,y)=\left(\frac{c(n+1)x^{n-1}}{2\nu}\right)^{\frac{1}{2}}y,\ \psi(x,y)=\left(\frac{2\nu cx^{n+1}}{(n+1)}\right)^{\frac{1}{2}}f(\eta,\tau),$$

$$T=T_\infty+(T_w-T_\infty)g(\eta,\tau)$$

where the subscript η denotes partial derivative with respect to η and τ is the dimensionless time *ct*. we seek the boundary conditions as eq. (4) and (5)

In terms of ordered pair (η,τ),

$$(1-\phi)^{-2.5}f_{\eta\eta\eta}+\left((1-\phi)+\phi\frac{\rho_s}{\rho_f}\right)(ff_{\eta\eta}-\beta f_\eta^2) - \left(M+\frac{(1-\phi)^{-2.5}}{k_p}\right)f_\eta-\left((1-\phi)+\phi\frac{\rho_s}{\rho_f}\right)f_{\eta\tau}=0 \quad (16)$$

$$\left(\frac{\alpha_{nf}}{\alpha_f}+R\right)f_{\eta\eta}+Pr\left((1-\phi)+\phi\frac{(\rho c_p)_s}{(\rho c_p)_f}\right)(g_\eta f-f_\eta g) - \left((1-\phi)+\phi\frac{\rho_s}{\rho_f}\right)g_\tau=0 \quad (17)$$

The boundary condition will reduce into:

$f(0,\tau)=0, f'(0,\tau)=\lambda+\gamma f''(0,\tau)+\delta f'''(0,\tau), g(0,\tau)=1$ (18)

$f'(\infty,\tau)\to 0$, $g(\infty,\tau)\to 0$ (19)

To show the stability of the solution, we set $f=f_0(\eta)$ and $g=g_0(\eta)$, which satisfying the boundary value problem (6-9), we suppose that

$$f(\eta,\tau)=f_0(\eta)+e^{-\sigma\tau}F(\eta,\tau) \quad (20)$$

$$g(\eta,\tau)=g_0(\eta)+e^{-\sigma\tau}G(\eta,\tau) \quad (21)$$

where σ is an unknown eigenvalue parameter, while $F(\eta,\tau)$ and $G(\eta,\tau)$ are small relative to $f_0(\eta)$ and $g_0(\eta)$. Substituting (20) and (21) into (16-19), and after linearizing problem, we obtain the following equations

$$(1-\phi)^{-2.5}F_{\eta\eta\eta}+\left((1-\phi)+\phi\frac{\rho_s}{\rho_f}\right)(f_0F_{\eta\eta}+Ff_0''-2\beta f_0'F_\eta) - \left(M+\frac{(1-\phi)^{-2.5}}{k_p}\right)f_\eta+\left((1-\phi)+\phi\frac{\rho_s}{\rho_f}\right)(\sigma F_\eta-F_{\eta\tau})=0 \quad (22)$$

$$\left(\frac{\alpha_{nf}}{\alpha_f}+R\right)G_{\eta\eta}+Pr\left((1-\phi)+\phi\frac{(\rho c_p)_s}{(\rho c_p)_f}\right)(f_0G_\eta+Fg_0'-f_0'G - F_\eta g_0)+\left((1-\phi)+\phi\frac{\rho_s}{\rho_f}\right)(\sigma G-G_\tau)=0 \quad (23)$$

Subject to boundary condition

$F(0,\tau)=0, F'(0,\tau)=\lambda+\gamma F''(0,\tau)+\delta F'''(0,\tau), G(0,\tau)=1$ (24)

$F'(\infty,\tau)\to 0$, $G(\infty,\tau)\to 0$ (25)

Now, we investigate the stability of the steady Nanofluid flow and temperature transfer solution $f_0(\eta)$ and $g_0(\eta)$ by setting $\tau=0$, and hence $F=F_0(\eta)$ and $G=G_0(\eta)$

in (22-23) to identify initial growth or decay of the solution (20) and (21). To test our numerical procedure we have to solve the following linear eigenvalue problem:

$$(1-\phi)^{-2.5}F_0'''+\left((1-\phi)+\phi\frac{\rho_s}{\rho_f}\right)(f_0F_0''+F_0f_0''-2\beta f_0'F_0')\ -$$

$$\left(M+\frac{(1-\phi)^{-2.5}}{k_p}\right)F_0'+\left((1-\phi)+\phi\frac{\rho_s}{\rho_f}\right)(\sigma F_0')=0 \qquad (26)$$

$$\left(\frac{\alpha_{nf}}{\alpha_f}+R\right)G_0''+Pr\left((1-\phi)+\phi\frac{(\rho c_p)_s}{(\rho c_p)_f}\right)(f_0G_0'+F_0g_0'-$$

$$f_0'G_0-F_0'g_0)+\left((1-\phi)+\phi\frac{\rho_s}{\rho_f}\right)(\sigma G_0)=0 \qquad (27)$$

Subject to boundary condition

$$F_0(0)=0,\ F_0'(0)=\lambda+\gamma F_0''(0)+\delta F_0'''(0),\ G_0(0)=1$$

$$F_0'(\infty)\to 0,\ G_0(\infty)\to 0 \qquad (28)$$

Using the numerical values of $F(\eta)$ and $G(\eta)$, Eqs. (26-28) are obtained. Solutions give an infinite set of eigen-values $1<\sigma 2<\sigma 3<\cdots$, if the smallest eigen-value $\sigma 1$ is positive, then there is an initial decay of disturbances and the flow is stable. On the other hand when $\sigma 1$ is negative, there is an initial growth of disturbances and the flow is unstable.

The physical parameters on boundary flow problem are the local skin friction coefficient C_f and Nusselt number Nu, which are formulated as

$$Cf_x=2(1-\phi)^{-2.5}Re_x^{-\frac{1}{2}}f''(0),$$

$$Nu=-2\frac{\alpha_{nf}}{\alpha_f}Re_x^{-\frac{1}{2}}g'(0),$$

where $Re_x=\dfrac{u_w x}{\nu(n+1)}$ is local Reynold number, for $\phi=1$, we get C_f and Nu fluid flow without nanoparticle.

3. Figures and Tables

In this segment, numerical outcomes for velocity and temperature field are elaborated through graphs. The computations are performed to study the impact of numerous physical flow parameters that describe the flow characteristics.

We have taken four kinds of nanoparticles i.e., Copper (Cu), Titanium oxide (TiO_2), Aluminum dioxide (Al_2O_3), silver (Ag) with water as a base fluid. Table 1 shows the thermo physical properties of water and the elements Cu, Al_2O_3, Ag and TiO_2. During the stability analysis, it is

Table 1. Material properties.

Materials	ρ (kg/m^3)	c_p (J/kgK)	α (W/mk)
Pure Water (H_2O)	997.1	4179	0.613
Copper (Cu)	8933	385	401
Alumina (Al_2O_3)	3970	765	40
Titanium oxide (TiO_2)	4250	686.2	8.9538
Silver (Ag)	10500	234	429

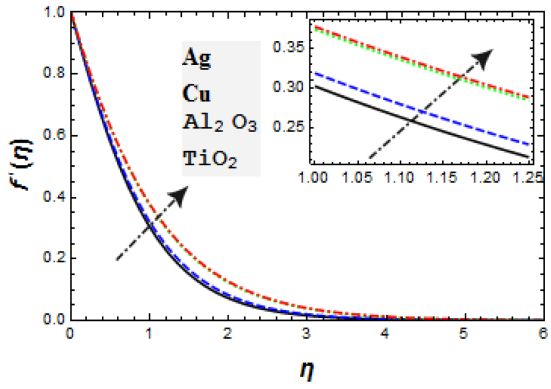

Fig. 1. (Color online) Velocities distribution $f'(\eta)$.

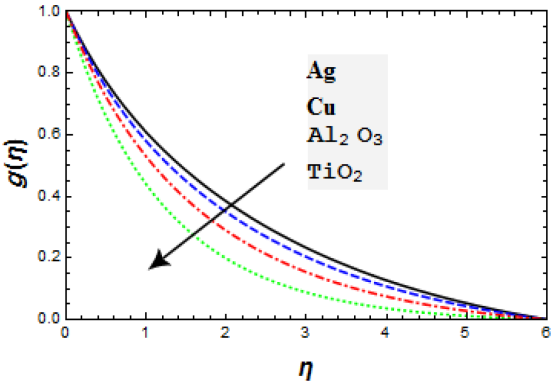

Fig. 2. (Color online) Temperature distribution $g(\eta)$.

Table 2. Smallest Eigenvalue for different value of λ.

λ	Silver (Ag)		Copper (Cu)		Alumina (Al_2O_3)		Titanium oxide (TiO_2)	
−0.25	0.3727	−0.1788	0.3514	−0.1621	0.1899	−0.1096	0.1873	−0.0999
−0.30	0.1982	−0.1122	0.1873	−0.0976	0.1103	−0.0692	0.1070	−0.0653
−0.35	0.1012	−0.0712	0.0962	−0.0466	0.0513	−0.0135	0.0497	−0.0127
−0.37	0.0732	−0.0133	0.0631	−0.0093	0.0023	−0.0038	0.0011	−0.0031

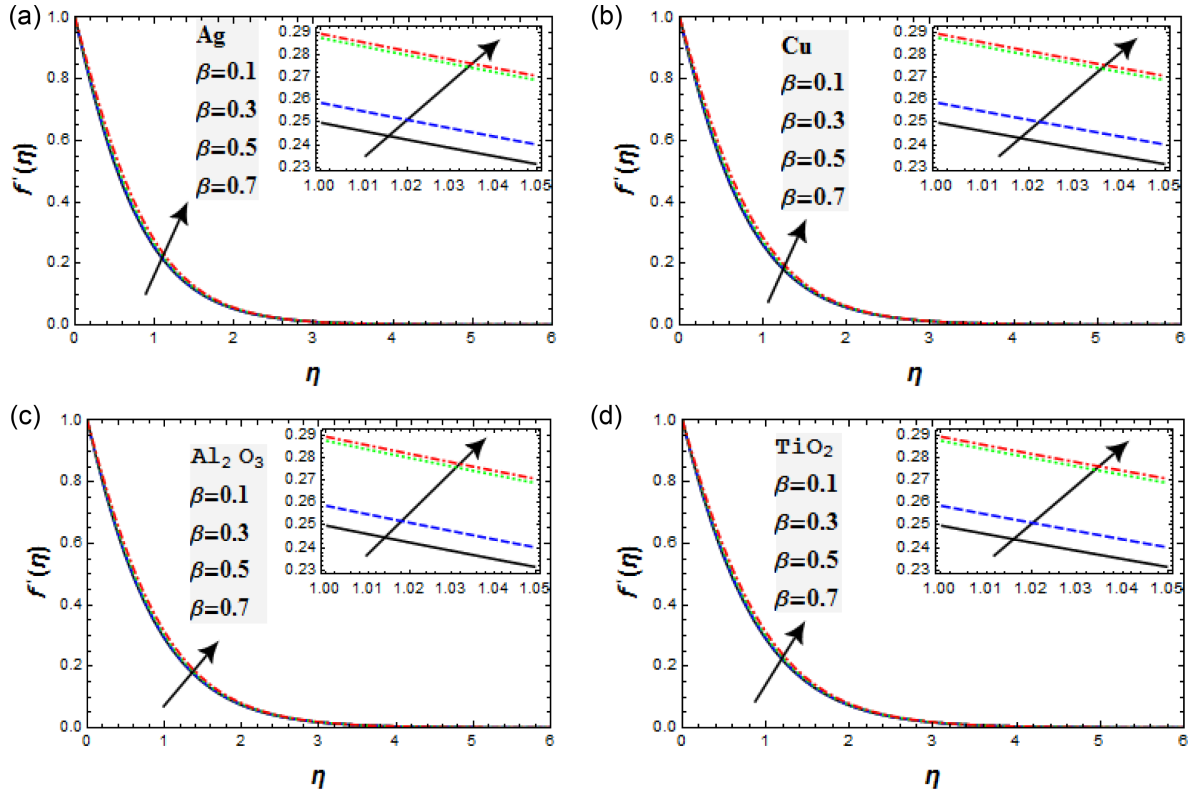

Fig. 3. (Color online) (a-d) Velocity of nano fluids for various values of β.

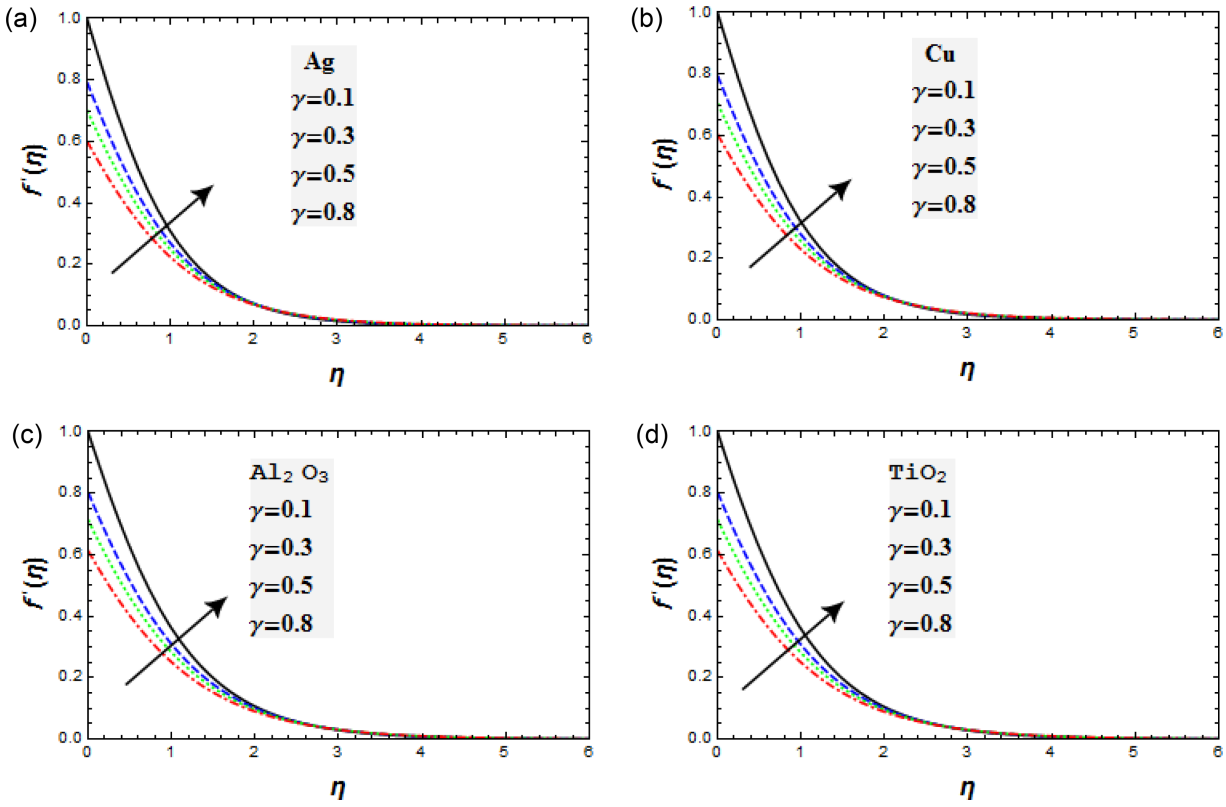

Fig. 4. (Color online) (a-d) Velocity of Nanofluid for numerous values of γ.

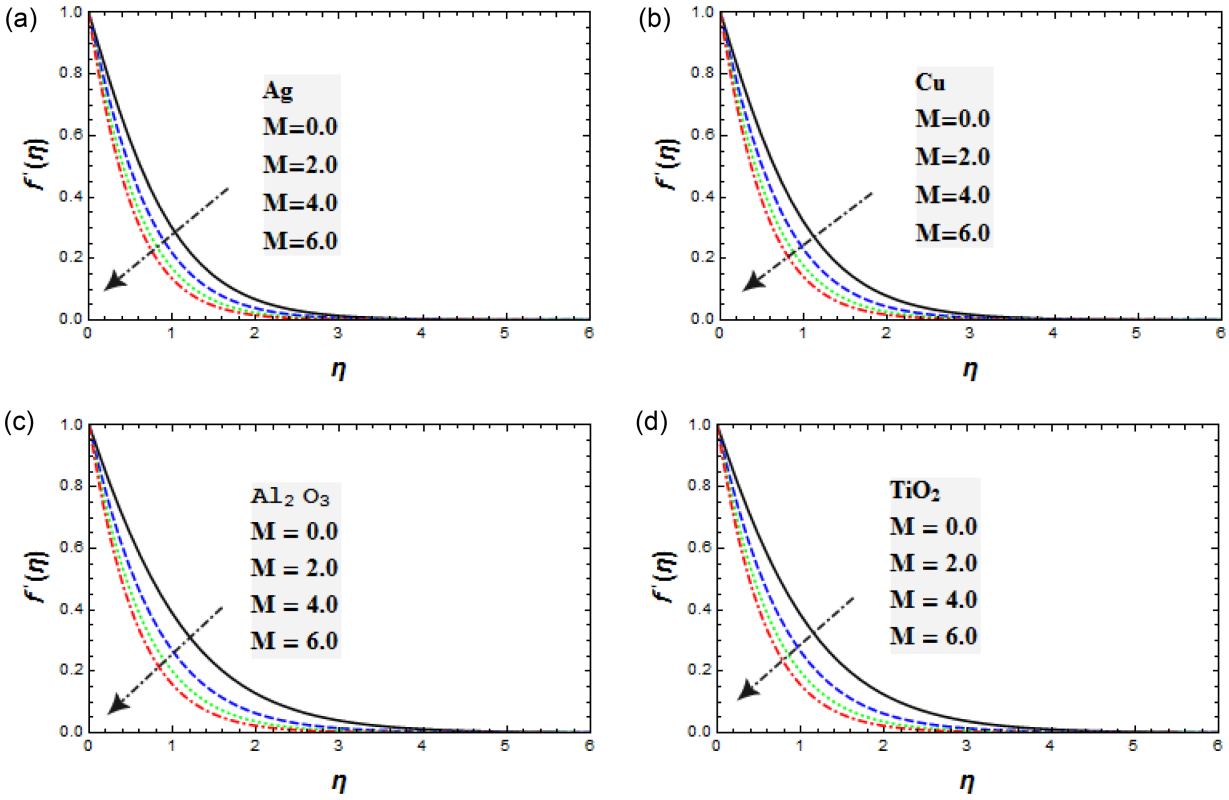

Fig. 5. (Color online) (a-d) Velocity of Nanofluid for numerous values of *M*.

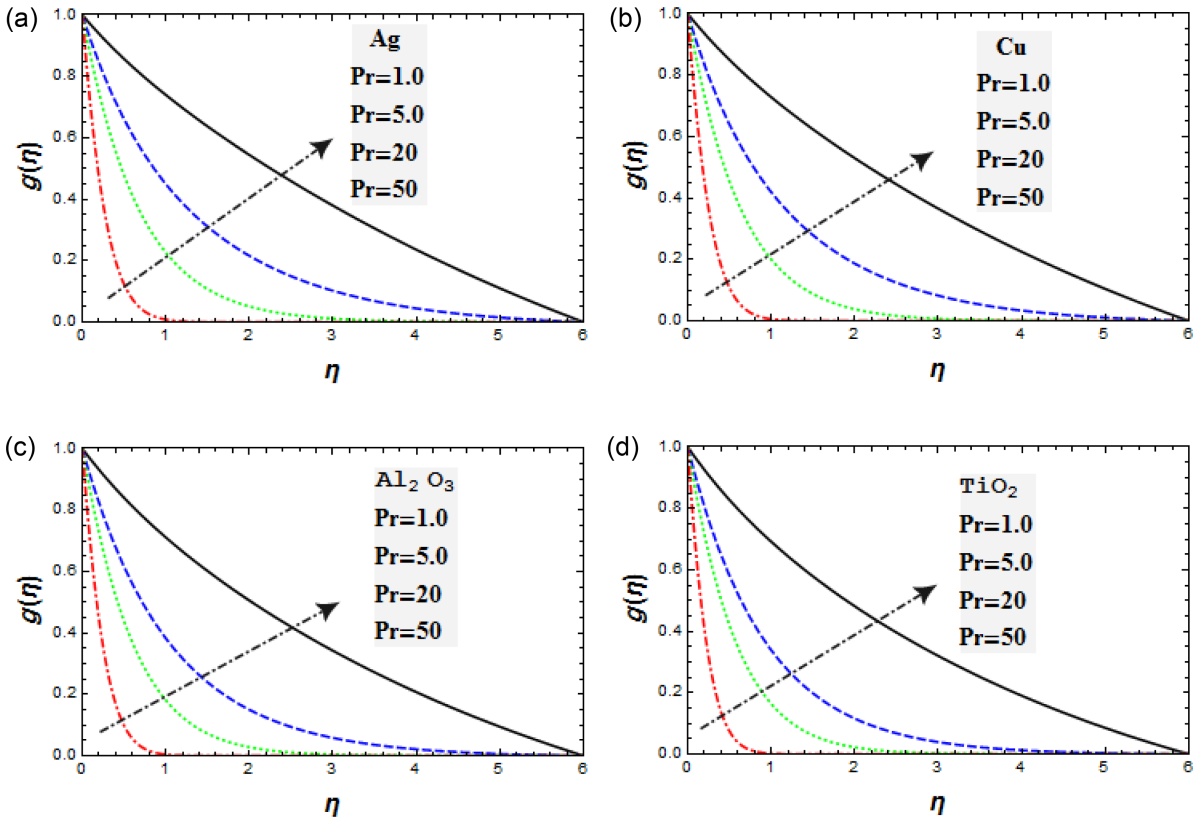

Fig. 6. (Color online) (a-d) Temperature of Nanofluid for various values of *Pr*.

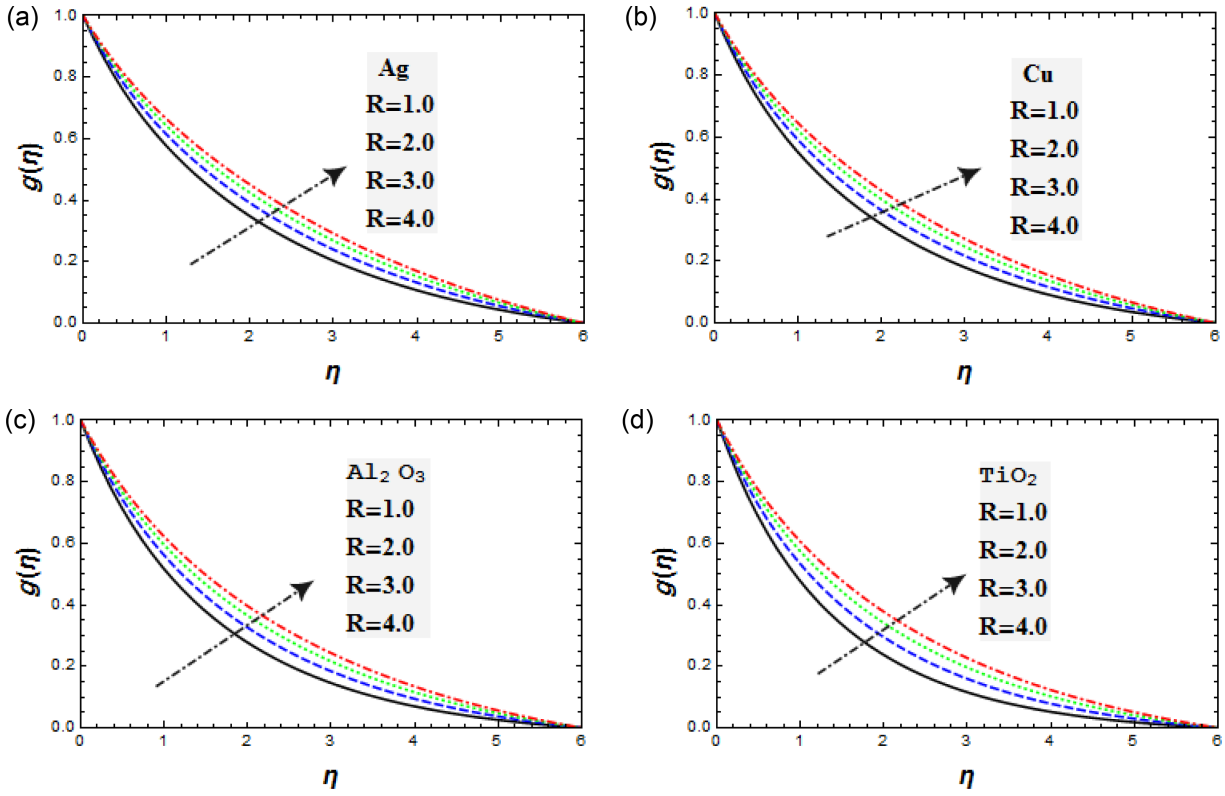

Fig. 7. (Color online) (a-d) Temperature of Nanofluid for various values of *R*.

seen that for $\lambda > 0$ (stretching sheet) the solution is stable. Whereas, $\lambda < 0$ (Shrinking sheet) for some values of parameter dual solution emerges. Smallest eigenvalues are obtained for both the solutions it is observed that the lower branch solutions have negative smallest Eigenvalue, and upper branch has positive eigenvalues. So, the upper branch of the solution is physically stable. Smallest eigenvalues calculated for different values of $\lambda < 0$ for all nanoparticles are shown in Table 2. Figure 1 shows the velocity distribution $f'(\eta)$ of nano-particles. It is noted that silver gain maximum velocity as compared to other nanoparticles. Figure 2 shows temperature distribution $g(\eta)$ in which silver has minimum temperature distribution as compared to others Nano-particles. Figure 3(a-d) illustrate that the velocity profile of silver, copper, Aluminum di oxide and Titanium with various values of power index β. It is noted that when values of β increases, the velocity of Nanofluid also increased. Figure 4(a-d) shows the velocity profile of Nanofluid with different values of γ. It shows that when values of γ increases, the velocity of Nanofluid is also increased. Figure 5(a-d) shows the velocity profile of Nanofluid with different values of magnetic parameter M. It shows that when values of M increases, the velocity profile of Nanofluid decreases. Figure 6(a-d) pointed out that temperature for various value of *Pr*. It is found that as the *Pr* increases, the temperature is also increased. Figure 7(a-d) shows the consequence of radiation parameter R on temperature distribution. It shows that when the values of R is increased, the temperature is also increasing.

References

[1] M. Sheikholeslami, M. M. Rashidi, T. Hayat, and D. D. Ganji, Journal of Molecular Liquids **218**, 393 (2016).
[2] T. Hayat, N. Aslam, A. Alsaedi, and M. Rafiq, International Journal of Heat and Mass Transfer **115**, 1033, (2017).
[3] T. Hayat, S. Ahmad, M. I. Khan, and A. Alsaedi, Physica B: Condensed Matter **537**, 116 (2018).
[4] S. U. S Choi, J. Heat Transfer **131**, 033106 (2009).
[5] K. Khanafer, K. Vafai, and M. Lightstone, Int. J. Heat Mass Transfer **46**, 3639 (2003).
[6] J. A. Eastman, S.U. S. Choi, S. Li, W. Yu, and L. J. Thompson, Appl. Phys. Lett. **78**, 718 (2001).
[7] Q. Li, Y. Xuan, and J. Wang, J. Heat Transfer **125**, 151 (2003).
[8] M. Sheikholeslami, T. Hayat, and A. Alsaedi, International Journal of Heat and Mass Transfer **106**, 745 (2017).
[9] T. T. Baby, and S. Ramaprabhu J. Appl. Phys. **108**,

124308 (2010).
[10] N. Bachok, A. Ishak, and I. Pop, Int. J. Therm. Sci. **49**, 1663 (2010).
[11] O. D. Makinde and A. Aziz, Int. J. Therm. Sci. **50**, 1326-1332 (2011).
[12] A. Zeeshan, A. Majeed, and R. Ellahi, J. Mol. Liq. **215**, 549 (2016).
[13] R. Ellahi, M. Hassan, and A. Zeeshan, Asia-Pacific J. of Chem. Eng. **11**, 179 (2016).
[14] M. M. Rashidi, S. Abelman, and N. F. Mehr, Int. J. Heat Mass Transfer **62**, 515 (2013).
[15] M. Sheikholeslami and R. Ellahi, Int. J. Heat Mass Transfer **89**, 799 (2013).
[16] T. Hayat, A. Aziz, T. Muhammad, and B. Ahmad, J. Magn. Magn. Mater. **408**, 99 (2016).
[17] B. Ganga, S. M. Y. Ansari, N. V. Ganesh, and A. A. Hakeem, J. of the Nigerian Math. Soc. **34**, 181 (2015).
[18] A. Majeed, A., Zeeshan, and R. Ellahi, J. Mol. Liq. **223**, 528 (2016).
[19] F. Mabood and W. A. Khan, J. Mol. Liq. **219**, 216 (2016).
[20] R. Ellahi, M. Hassan, and A. Zeeshan, Mech. Adv. Mater. Struct. **24**, 1231 (2017).
[21] A. Zeeshan, M. Hassan, R. Ellahi, and M. Nawaz, Proc. Instit. Mech. Eng. J. of Proc. Mech. Eng. **231**, 871 (2017).
[22] N. Shehzad, A. Zeeshan, R. Ellahi, and K. Vafai, J. Mol. Liq. **222**, 446 (2016).
[23] M. Turkyilmazoglu, Comput. Fluids **71**, 426 (2016).
[24] N. C. Roşca and I. Pop, Eur. J. Mech. B. Fluids **48**, 115 (2014).
[25] T. Hayat, M. I. Khan, S. Qayyum, A. Alsaedi, and M. I. Khan, Physics Letters A **382**, 749 (2018).
[26] T. Hayat, F. Shah, A. Alsaedi, and Z. Hussain, Results in Physics **7**, 2497 (2017).
[27] M. Khan, W. Ahmed, M. I. Khan, T. Hayat, and A. Alsaedi, Physica B: Condensed Matter **534**, 113 (2018).
[28] R. Nazar, A. Noor, K. Jafar, and I. Pop, International Journal of Mathematical, Computational, Physical, Electrical and Computer Engineering **8**, 782 (2014).